Japanese Journal of Applied Physics

Frequency Metrology with Optical Lattice Clocks

To cite this article: Feng-Lei Hong and Hidetoshi Katori 2010 *Jpn. J. Appl. Phys.* **49** 080001

Frequency Metrology with Optical Lattice Clocks

Feng-Lei Hong[1,3*] and Hidetoshi Katori[2,3†]

[1] National Metrology Institute of Japan (NMIJ), National Institute of Advanced Industrial Science and Technology (AIST), Tsukuba, Ibaraki 305-8563, Japan
[2] Department of Applied Physics, Graduate School of Engineering, The University of Tokyo, Bunkyo, Tokyo 113-8656, Japan
[3] CREST, Japan Science and Technology Agency, Kawaguchi, Saitama 332-0012, Japan

Received March 10, 2010; accepted April 13, 2010; published online August 20, 2010

The precision measurement of time and frequency is of great interest for a wide range of applications, including fundamental science and technologies that support broadband communication networks and the navigation with global positioning systems (GPSs). The development of optical frequency measurement based on frequency combs has revolutionized the field of frequency metrology, especially research on optical frequency standards. The proposal and realization of the optical lattice clock have further stimulated studies in the field of optical frequency metrology. Optical carrier transfer using optical fibers has been used to disseminate optical frequencies or compare two optical clocks without degrading their stability and accuracy. In this paper, we review the state-of-the-art development of optical frequency combs, standards, and transfer techniques with emphasis on optical lattice clocks. We address recent results achieved at the University of Tokyo and the National Metrology Institute of Japan in respect of frequency metrology with Sr and Yb optical lattice clocks.

DOI: 10.1143/JJAP.49.080001

1. Introduction

Fifty years ago, clocks were under the control of astronomers because the "second" was defined in terms of the period of revolution of the earth around the sun. Since the invention of the atomic clock, physicists have taken over the role of timekeeping. The first Cs atomic clock made by Essen[1)] in 1957 at the National Physical Laboratory (NPL) had an uncertainty of 1×10^{-10}, which was about one order of magnitude smaller than that of the second realized with the definition using the revolution of the earth. Since then, physicists have been working hard to improve atomic clocks. With the optical pumping method for selecting atomic states, the uncertainty of the Cs clock was reduced to the 10^{-14} level. By using the laser cooling technique, an atomic fountain Cs clock with an uncertainty of $\sim 4 \times 10^{-16}$ has been realized.[2)] With the invention of an optical frequency comb,[3–5)] atomic clocks using optical transitions have been developed rapidly. One of the most promising candidate optical clocks is the single-trapped-ion clock, which has been studied for more than 30 years.[6)] State-of-the-art experiments have achieved an uncertainty of 10^{-17} with single trapped Hg^+ and Al^+.[7)] As a new possibility, an optical lattice clock was proposed in 2001,[8)] which may improve the quantum projection noise limit in the single-trapped-ion clock. After successful demonstrations with Sr atoms,[9,10)] optical lattice clocks are now being studied using Sr,[10–12)] Yb,[13,14)] and Hg[15,16)] atoms by nearly 20 groups worldwide. Although at present the uncertainty realized with lattice clocks is 1.5×10^{-16},[17)] it is expected to reach one part in 10^{18}.[16,18)] The rapid development of optical lattice clocks has pushed forward the entire field of frequency metrology, especially in the optical area including optical frequency standards, measurements, comparisons, and transfer. In this article, we review the recent development of optical frequency metrology, together with detailed description of the achievement with the Sr and Yb optical lattice clocks at the University of Tokyo and the National Metrology Institute of Japan (NMIJ).

*E-mail address: f.hong@aist.go.jp
†E-mail address: katori@amo.t.u-tokyo.ac.jp

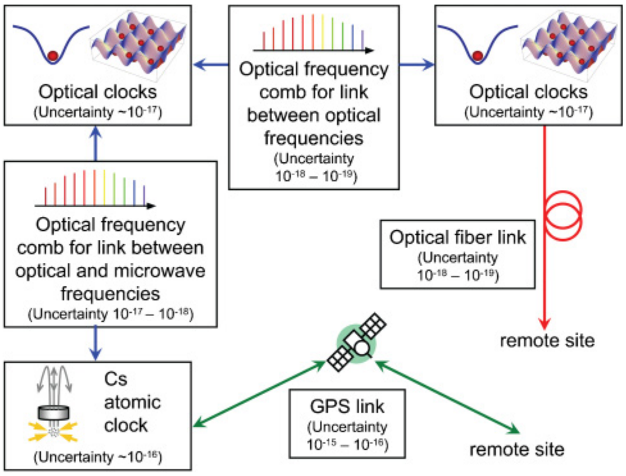

Fig. 1. (Color online) Standards and measurement tools involved in optical frequency metrology. The listed uncertainties are the achieved uncertainties of the standards and measurement tools.

2. Basics of Optical Frequency Metrology

Figure 1 shows the standards and measurement tools involved in optical frequency metrology. Optical combs are used to link optical and microwave frequencies with uncertainties of 10^{-17}–10^{-18},[19,20)] and to link optical frequencies with uncertainties of 10^{-18}–10^{-19}.[21)] Microwave frequency can be transferred using a global positioning system (GPS) link with uncertainties of 10^{-15}–10^{-16},[22,23)] while optical frequency can be transferred using an optical fiber link with uncertainties of 10^{-18}–10^{-19}.[24,25)]

2.1 Optical frequency comb

At the end of the 20th century, it was demonstrated that mode-locked femtosecond lasers can be used to measure the absolute frequency of an optical frequency standard using a Cs atomic clock as a frequency reference.[3–5)] A frequency comb obtained by injecting the light of a Kerr-lens mode-locked Ti:sapphire (Ti:S) laser into a photonic crystal fiber (PCF)[26,27)] can cover more than one octave of optical frequencies (Ti:S comb, 500–1100 nm), enabling the direct measurement of the carrier-envelope offset (CEO) frequency of the femtosecond comb with an f-to-$2f$ interferometer.[5] The frequency comb has been confirmed to be a reliable tool for optical frequency comparisons with an uncertainty of 10^{-19}.[21] Furthermore, the frequency stability of the microwave signal converted from an optical frequency standard using the frequency comb has been demonstrated to be below 2×10^{-16} at an averaging time of 1 s and about 3×10^{-19} at 6.5×10^4 s.[20] For high-precision frequency measurement, the combination of a hydrogen maser (H-maser) and a Cs fountain clock is usually used as a frequency reference source for obtaining both good short-term stability and accuracy.

Toward practical applications, a frequency comb based on an Er-doped mode-locked fiber laser (fiber comb) has attracted considerable attention.[28] Instead of expensive and bulky solid-state pump lasers for the Ti:S comb, the fiber comb uses low-cost and compact diode lasers as pump sources. Furthermore, the difficulty in the long-term operation of the Ti:S comb caused by the instability of the coupling efficiency of the PCF can be resolved in the fiber comb because the highly nonlinear fiber for spectrum broadening is spliced onto the laser fiber. Frequency stabilization and absolute frequency measurement have also been realized with turnkey all-fiber systems.[29,30] Furthermore, a fiber comb was demonstrated to measure optical frequencies continuously for more than one week.[31] One problem of fiber combs was their larger phase noise compared with Ti:S combs, which results in a broad optical linewidth up to several hundreds of kHz.[28] With proper design of the mode-locked fiber laser and active feedback by controlling pump-diode current, phase noise could be reduced, thereby decreasing the linewidth to less than 1 Hz.[32–34] With such improvements and inherently low-cost and easy-to-use characters, fiber combs are now widely used in applications including frequency measurement, laser frequency control, precision measurements, and sensing. For example, a fiber comb is proposed to be used in advanced accelerators for precise timing control of electron bunches.[35]

The Ti:S and fiber combs completely cover a wavelength range from 500 to 2000 nm. For wavelengths shorter than 500 nm, one possible approach is to use the broadened spectrum obtained by injecting the second-harmonic generation (SHG) of a mode-locked fiber laser into a PCF.[28] UV combs have been generated using high-harmonic generation at wavelengths shorter than 100 nm.[36,37] On the other hand, for wavelengths longer than 2000 nm, the sum-frequency generation[38–40] and difference-frequency generation[41,42] of an optical frequency comb have been demonstrated to be effective methods. With the enlarged comb wavelength range, optical frequency combs have been demonstrated to have extensive applications, such as breath analysis,[43] astronomical observations.[44]

2.2 Optical frequency standard

Lasers frequency-stabilized to the transitions of atoms, ions, and molecules were recommended by the International Committee for Weights and Measures (CIPM) as optical frequency standards for metrology applications.[45,46] Among these recommendations, optical standards based on single trapped ions[6] and ultracold neutral atoms in free fall[47,48] provided record levels of performance that approach those of the best Cs fountain clocks early in this century. Both of these single-ion and neutral-atom standards have advantages and disadvantages. The advantages of the single-ion standard are its long interaction time and Lamb–Dicke confinement[49] for the suppression of the first-order Doppler-shift, while the disadvantage is its clock stability being limited by the quantum projection noise provided by the single ion. Although the neutral-atom standards that interrogate millions of atoms well surpass the single-ion clock in stability, their uncertainties are severely degraded by residual Doppler shifts and atomic collisions, which prevent them from reaching 10^{-15} uncertainties.[50] These tradeoffs in the two traditional approaches to developing optical clocks inspired the optical lattice clock scheme, as detailed in §3.

Here, we outline several main single-ion frequency standards as follows:

1) $^{199}Hg^+$ standard: The uncertainty of the absolute frequency measurement is 7×10^{-16}.[51] The frequency stability is 2.8×10^{-16} at 100 s and the reproducibility is 1.9×10^{-17}, evaluated using optical-to-optical comparison.[7]
2) $^{88}Sr^+$ standard: The uncertainty of the absolute frequency measurement is 3.4×10^{-15}.[52] This was limited by the ac stark effect and the H-maser used in the frequency measurement.
3) $^{171}Yb^+$ standard: The uncertainty of the absolute frequency measurement is 1.1×10^{-15}.[53] This was limited by the quadrupole shift due to the interaction of stray electric field and black-body radiation.
4) $^{27}Al^+$ standard: The uncertainty of the frequency ratio of the two optical clocks (ν_{Al^+}/ν_{Hg^+}) is 5.2×10^{-17}.[7] The frequency stability is 2.8×10^{-16} at 100 s and the clock uncertainty is 8.6×10^{-18}, evaluated using two Al^+ clocks.[54]

2.3 Optical frequency transfer

The precision of the conventional frequency transfer and comparison method needs to be improved so as to meet the high stability requirement of optical clocks. The ubiquitous fiber optic network enables us to transfer frequencies with an extremely low phase noise.[55,56] There are two methods to transfer frequencies using optical fibers. In both cases, active phase noise cancellation is necessary because of the additional phase noise due to the optical length fluctuations of the delivering fibers caused by mechanical or temperature variations.

1) Microwave frequencies have been faithfully transmitted over a modulated optical signal at 1.5 µm with a fractional frequency stability of 5×10^{-15} at 1 s through an 86 km fiber.[57]

2) Instead of using the modulation on optical signals, one can use the optical carrier signal with the optical phase information to achieve stability that is several orders of magnitude higher. This very stable optical carrier transfer can be used to compare two optical clocks without degrading their stability and accuracy.[58] Results have been reported for tests on coherent optical frequency transfer with residual frequency instabilities of 1×10^{-17} through a 32 km fiber[24] and 2×10^{-16} through a 251 km fiber[25] at 1 s. A precision frequency measurement of a Sr optical lattice clock has been demonstrated on the basis of an optical carrier transfer over a

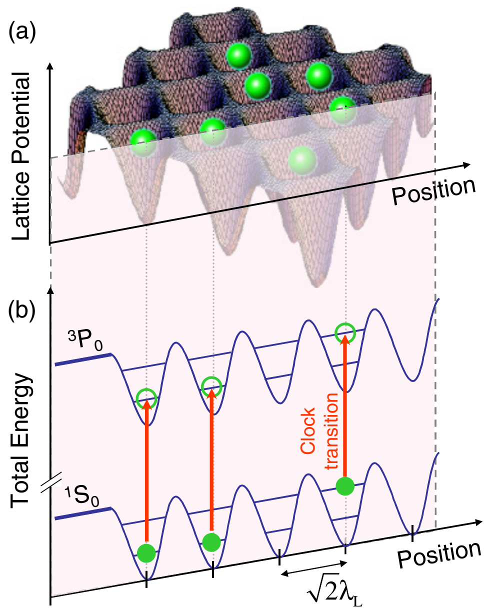

Fig. 2. (Color online) Realization of an optical lattice clock. (a) The spatial interference pattern of lasers creates a lattice potential that confines atoms in a region much smaller than the optical wavelength λ_L. (b) Atoms are excited on the $^1S_0$–$^3P_0$ clock transitions, where the $^1S_0$ and $^3P_0$ states are equally energy-shifted by the lattice potential.

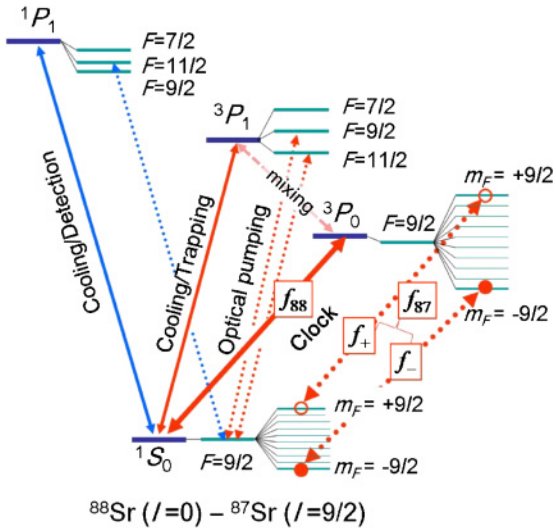

Fig. 3. (Color online) Energy levels for ^{88}Sr and ^{87}Sr atoms. Spin-polarized ultracold ^{87}Sr atoms were prepared by optical pumping on the $^1S_0(F = 9/2)$–$^3P_1(F = 9/2)$ transition at $\lambda = 689$ nm with circularly polarized light. The first-order Zeeman shift and the vector light shift on the clock transition at $\lambda = 698$ nm were eliminated by averaging the transition frequencies $f_\pm$.

120-km long-haul fiber network composed of installed rural and urban telecom fibers.[59,60)]

3. Optical Lattice Clock

An "optical lattice clock"[8)] was proposed to realize a high clock stability and a high accuracy simultaneously. The scheme uses millions of neutral atoms trapped in an optical lattice (see Fig. 2), where the light field perturbation is canceled out by properly designing the light shift potentials. The subwavelength localization of atoms in each lattice site suppresses the first-order Doppler-shift[49)] and collisional shift, while it provides a long interrogation time; therefore the scheme shares the advantages of the two existing clock schemes described in §2.2. After introducing the key concept of "light shift cancellation" realized by the "magic wavelength", a more precise definition of the "magic wavelength" including the multipolar interactions between atoms and lattice fields, and the applicability of the scheme are addressed.

3.1 Light shift cancellation

In designing atomic clocks, utmost elimination of perturbations on electronic states and of motional effects has been considered to be the heart of the enterprise. In this viewpoint, singly trapped ions in an RF quadrupole field[6)] and ultracold neutral atoms in free fall[48)] are expected to be the best realization of atomic clocks. In striking contrast with these traditional approaches, the optical lattice clocks utilize well-controlled perturbation applied on the atoms.

In general, the electronic states of atoms trapped in optical lattices are significantly energy-shifted by the so-called light shifts; hence, the system is far from the traditional criteria for atomic clocks. However, if the lattice field provides the same amount of light shift to the two states used for the clock transition, the light shift perturbation can be eliminated.[61)] The clock transition frequency of atoms exposed to a lattice laser (see Fig. 2) with an electric field amplitude E is given by the sum of the unperturbed transition frequency ν_0 and the differential light shift ν_{ac}. In the electric dipole approximation, it is given by

$$\begin{aligned}\nu(\lambda_L, \mathbf{e}_L) &= \nu_0 + \nu_{ac}\\ &= \nu_0 - \frac{\Delta\alpha(\lambda_L, \mathbf{e}_L)}{2h} E^2(\lambda_L, \mathbf{e}_L) + O(E^4), \qquad (1)\end{aligned}$$

where h is the Planck constant and $\Delta\alpha(\lambda_L, \mathbf{e}_L) = \alpha_u(\lambda_L, \mathbf{e}_L) - \alpha_l(\lambda_L, \mathbf{e}_L)$ is the difference between the (electric-dipole) polarizabilities of the upper and lower states that depend both on the lattice laser wavelength λ_L and the polarization vector $\mathbf{e}_L$. By tuning polarizabilities to satisfy $\Delta\alpha(\lambda_L, \mathbf{e}_L) = 0$ employing laser wavelength or polarization, the observed atomic transition frequency ν will be equal to ν_0 independent of lattice laser intensity ($\propto E^2$), as long as the higher-order corrections $O(E^4)$ are negligible. Earlier experiments[61,62)] on light shift cancellation on the $^1S_0$–$^3P_1$ transition, however, led us to infer that the coupling of the $J = 1$ state and the light-polarization $\mathbf{e}_L$ causes a vector light shift, which can be a fatal problem in pursuing atomic-clock level accuracy, because of the difficulty in the precise control of the light polarization.

To provide the light shift cancellation condition solely by the laser wavelength λ_L or equivalently by its frequency $\nu_L = c/\lambda_L$, which is the most precisely measurable quantity in physics, it would be ideal to use the $J = 0$ state that exhibits a scalar light shift. However, as the $J = 0 \rightarrow J = 0$ transition is completely forbidden, a slight admixture of the $J = 1$ state is necessary to allow the transition. In our initial proposal,[8)] therefore, we took the $5s^2\ ^1S_0(F = 9/2) \rightarrow 5s5p\ ^3P_0(F = 9/2)$ transition of ^{87}Sr as the clock transition, where its nuclear spin of $I = 9/2$ introduces hyperfine mixing to introduce a 1 mHz transition rate (see Fig. 3). Alternatively, it is proposed to use the $^1S_0 \rightarrow {}^3P_0$ transition of atoms by applying a bias magnetic field that Zeeman-mixes the upper $^3P_0$ state with a nearby $J = 1$ state.[63)]

3.2 Quantum statistics of atoms and optical lattice geometry

In designing atomic clocks, the control and prevention of atomic interactions are another concern. The collisional frequency shift of atomic clocks operated with ultracold atoms is related to the mean field energy shift $\mathcal{E} = 4\pi\hbar^2 a n g^{(2)}(0)/m$ of the relevant electronic state, with the s-wave scattering length a, atomic density n, and atomic mass m. Here, $g^{(2)}(0)$ is the two-particle correlation function at a zero distance, which is zero for identical fermions and $1 \leq g^{(2)}(0) \leq 2$ for distinguishable or bosonic atoms. Hence, the collisional shifts are suppressed for ultracold fermions, while they are intrinsically unavoidable in bosons. The quantum statistical nature of atoms is determined by their total spins; that is, bosons have zero or integer spins and fermions have half-integer spins. In particular, for atoms with an even number of electrons that may have a $J = 0$ state suitable for optical lattice clocks, their nuclear spins I may be zero for bosons and $I \geq 1/2$ for fermions. Consequently, the total angular momentum $F = J + I$ of the clock states can be zero for bosonic atoms, but not for fermions, which causes coupling to the light polarization of the lattice field, as mentioned in §3.1.

Here, we consider two lattice geometries. A one-dimensional (1D) [see Fig. 4(a)] or 2D lattice composed of a single electric field vector may have spatially uniform light polarization. In contrast, a 3D lattice requires at least two electric field vectors; therefore, the synthesized field exhibits a polarization gradient that varies in space depending on the intensity profile of the lattice lasers. We discuss that these characteristics of light polarization lead to two optimal lattice clock configurations when combined with the quantum statistical properties of atoms.

3.2.1 1D optical lattice with spin-polarized fermions

Since their first demonstration,[9,10] optical lattice clocks were mostly realized by 1D optical lattices employing fermionic[10,12,64] or bosonic[65,66] isotopes. These experiments successfully demonstrated the advantage of optical lattice clocks at a 10^{-15} uncertainty by the Doppler free spectrum provided by the Lamb–Dicke confinement. However, collision shifts should exist in the 1D scheme with bosonic[67] or unpolarized fermionic[68] atoms because of the relatively high atomic densities of up to 10^{11} cm^{-3} in a single lattice site, which would surely dominate the uncertainty budget in the future.

In 1D optical lattice clocks with multiple atoms in each lattice site, the application of spin-polarized fermions[69,70] may minimize the collisional frequency shift by their quantum-statistical properties. Figure 4(a) shows the schematic diagram for the "spin-polarized" 1D optical lattice clock,[23] where the upward arrows correspond to spin-polarized fermionic atoms. An advantage of the 1D optical lattice is that the light field polarization is spatially uniform, which allows us canceling out the vector light shift[23] by alternately interrogating the transition frequencies $f_{\pm}$, corresponding to two outer Zeeman components $^1S_0(F, \pm m_F)$–$^3P_0(F, \pm m_F)$ of the clock transition (see Fig. 3). This vector light shift cancellation technique, which is discussed in detail in §4.2.2, also cancels out the Zeeman shift, thereby realizing virtual spin-zero atoms.

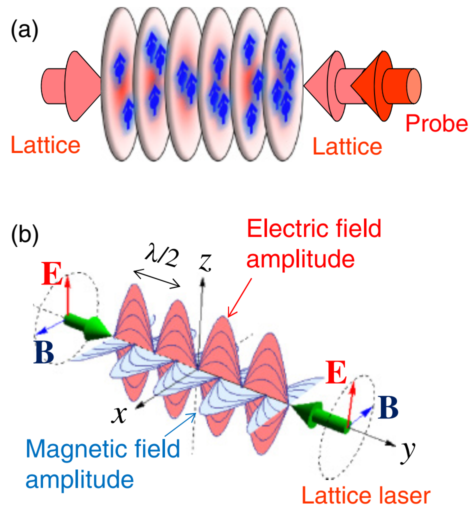

Fig. 4. (Color online) (a) A one-dimensional optical clock is realized by a standing wave of light tuned to the magic wavelength. Multiply trapped spin-polarized fermions in a single pancake potential may be protected from collisions by the Pauli blocking. (b) Electric and magnetic field amplitudes in a standing wave.

3.2.2 3D optical lattice with single-occupancy bosons

To suppress atomic collisions, the application of 3D optical lattices with less than a single atom in each lattice site, as shown in Fig. 2(a), may be effective as proposed initially.[8] However, as mentioned earlier, light polarization inhomogeneity inevitable in 3D optical lattices makes a vector light shift for atoms with its angular momentum $F \neq 0$ problematic, as the "vector light shift cancellation" technique is no longer applicable. From this viewpoint, the 3D lattice will be more suitable for bosonic atoms with scalar states ($J = 0$). Technically, it is more challenging to realize stable 3D optical lattices, as regards their position as well as local polarization, than 1D ones. One of the simple solutions is to apply "folded optical lattices",[71] where the 3D optical lattice consists of a single standing wave of light. In this configuration, the local polarization of lattice sites remains unchanged, as the two orthogonal electric field vectors oscillate in phase at the local lattice site.

The three-dimensional optical lattice clock has been demonstrated with bosonic ^{88}Sr atoms[72,73] for the first time. Its systematic uncertainties were investigated at 3×10^{-15} by referencing a spin-polarized 1D optical lattice clock with fermionic ^{87}Sr atoms.

3.3 Blue-detuned magic wavelength

To moderate the hyperpolarizability effects that cannot be canceled out at the (red-detuned) magic wavelength, a blue-detuned lattice that confines atoms in the intensity minima of the electric field seems promising. For Sr, such wavelengths are found on the blue side of the $5s^2\ ^1S_0$–$5s5p\ ^1P_1$ transition at 461 nm. A very far-off-resonance condition, however, is generally difficult to satisfy because the magic wavelength can only be found close to the transitions arising from the $5s5p\ ^3P_0$ state, as indicated in Fig. 5(a).

One such wavelength is found at $\lambda_L \approx 390$ nm on the blue side of the $5s5p\ ^3P_0$–$5s6d\ ^3D_1$ transition at 394 nm. For this magic wavelength, the laser intensity of $I_L = 10$ kW/cm^2 gives a trap depth of about 200 kHz, as indicated in

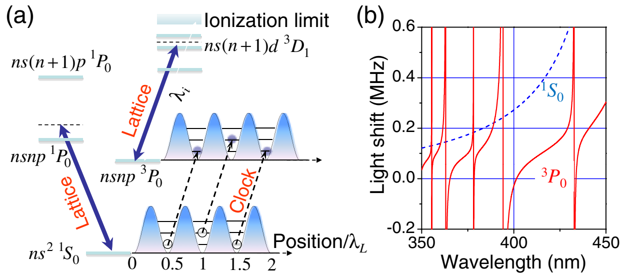

Fig. 5. (Color online) (a) Energy levels for alkaline-earth atoms relevant to blue magic wavelengths for the $^1S_0$–$^3P_0$ clock transition. By applying the lattice laser detuned slightly above the nearby state, $nsnp\ ^1P_1$ and $ns(n+1)d\ ^3D_1$, atoms can be trapped near the nodes of the standing wave. (b) The light shifts for the $^1S_0$ (dashed blue) and $^3P_0$ (solid red) states of Sr as a function of the lattice laser wavelength for a laser intensity of $I = 10\,\mathrm{kW/cm^2}$. Intersections of the curves indicate blue magic wavelengths, which include $\lambda_b \approx 360$ and 390 nm.

Fig. 5(b). The effective light intensity that atoms experience will be about 1/10 of the maximum intensity, as the atoms are trapped near the node of the standing wave. Assuming a trap depth of 10 μK, a fourth-order light shift [the last term in eq. (1)] is estimated to be 0.1 mHz, corresponding to a fractional uncertainty of 2×10^{-19}.[74] The blue magic wavelength is experimentally determined to be 389.889(9) nm[74] employing ^{87}Sr atoms trapped in the 1D optical lattice operated at the (red-detuned) magic wavelength of $\lambda_L = 813.4$ nm.

3.4 Multipolar interactions of atoms with lattice field and atomic-motion-insensitive wavelength

The optical lattice clocks operated at the blue magic wavelength appears to be ideal in view of the electric dipole (E1) interaction of atoms with a lattice laser field. However, when taking atomic multipolar interactions into account, things are not that simple. Consider, for example, the linearly polarized ($\|\mathbf{e}_z$) standing wave electric field $\mathbf{E} = \mathbf{e}_z E_0 \sin ky \cos \omega t$ with a wave number k and a frequency ω, as shown in Fig. 4(b). Following the Maxwell equation $\nabla \times \mathbf{E} = -(1/c)(\partial \mathbf{B}/\partial t)$ with c as the speed of light, the corresponding magnetic field is given by $\mathbf{B} = -\mathbf{e}_x E_0 \cos ky \sin \omega t$. This indicates that the electric and magnetic field amplitudes are one quarter of the wavelength $\lambda/4 = \pi c/(2\omega)$ out of phase in space. Consequently, the magnetic dipole (M1) interaction is largest at the nodes of the electric field. Furthermore, as the electric quadrupole (E2) interaction is proportional to the gradient of the electric field, the E2 interaction is also largest at the node of the electric field. Hence, the blue magic wavelength is not necessarily free of multipolar light shift perturbations.

The energy shift of atoms in the optical lattices is obtained by the second-order perturbation in E1, M1, and E2 interactions that vary as $V_{\mathrm{E1}} \sin^2 ky$, $V_{\mathrm{M1}} \cos^2 ky$, and $V_{\mathrm{E2}} \cos^2 ky$. As a result, it is no longer possible to perfectly match the total light shift in two clock states. For example, at the magic wavelength for the E1 interaction as discussed in §3.1, differential light shifts due to M1 and E2 interactions exist, which introduce an atomic-motion-dependent light shift because of their spatial mismatch with the E1 interaction.[75]

Although the contributions of the M1 and E2 interactions are 6–7 orders of magnitude smaller than that of the E1 interaction in optical lattice clocks in Sr,[18] they have a non-negligible contribution in pursuing the 1×10^{-18} level uncertainty. Therefore, a more precise definition of the magic wavelength, including multipolar interactions, is necessary. Assuming the differential polarizabilities of the E1, M1, and E2 interactions in the clock transition to be $\Delta\alpha_{\mathrm{E1}}(\lambda_{\mathrm{L}})$, $\Delta\alpha_{\mathrm{M1}}(\lambda_{\mathrm{L}})$, and $\Delta\alpha_{\mathrm{E2}}(\lambda_{\mathrm{L}})$, and the corresponding spatial distributions to be $q_{\mathrm{E1}}(\mathbf{r})$, $q_{\mathrm{M1}}(\mathbf{r})$, and $q_{\mathrm{E2}}(\mathbf{r})$, the transition frequency of atoms in the optical lattices can be given by

$$\nu(\lambda_{\mathrm{L}}) = \nu_0 - \frac{1}{2h}[\Delta\alpha_{\mathrm{E1}}(\lambda_{\mathrm{L}})q_{\mathrm{E1}}(\mathbf{r}) + \Delta\alpha_{\mathrm{M1}}(\lambda_{\mathrm{L}})q_{\mathrm{M1}}(\mathbf{r}) + \Delta\alpha_{\mathrm{E2}}(\lambda_{\mathrm{L}})q_{\mathrm{E2}}(\mathbf{r})]\,E^2, \tag{2}$$

which corresponds to eq. (1), but the 4th- and higher-order terms and light polarization dependences are omitted. One of the authors and the others have shown that one can eliminate atomic-motion-dependent light shift caused by multipolar interactions by choosing particular 3D optical lattice geometries that make them in phase or out of phase with respect to the spatial dependence of E1 interaction.[76] For example, in the case of a 1D lattice with the E1 spatial dependence $q_{\mathrm{E1}}(\mathbf{r}) = \sin^2 ky\,(= 1 - \cos^2 ky)$, the corresponding M1 and E2 interactions can be expressed as $q_{\mathrm{M1}}(\mathbf{r}) = q_{\mathrm{E2}}(\mathbf{r}) = \cos^2 ky = \Delta q - q_{\mathrm{E1}}(\mathbf{r})$ with $\Delta q = 1$. Therefore, by taking $\Delta\alpha_{\mathrm{EM}} \equiv \Delta\alpha_{\mathrm{E1}} - \Delta\alpha_{\mathrm{M1}} - \Delta\alpha_{\mathrm{E2}}$ and $\Delta\alpha_0 \equiv \Delta\alpha_{\mathrm{M1}} + \Delta\alpha_{\mathrm{E2}}$, [eq. (2)] can be rewritten as

$$\nu(\omega_{\mathrm{L}}) = \nu_0 - \frac{1}{2h}\Delta\alpha_{\mathrm{EM}}(\omega_{\mathrm{L}})q_{\mathrm{E1}}(\mathbf{r})E^2 - \frac{1}{2h}\Delta\alpha_0(\omega_{\mathrm{L}})\Delta q E^2, \tag{3}$$

where the second term on the right side varies in phase as the E1 interaction. This equation suggests the precise definition of the magic wavelength to be an "atomic-motion insensitive" wavelength. The last term provides a spatially constant offset typically of 10 mHz level and is solely dependent on the total laser intensity $\propto \Delta q E_0^2$ used to form the lattice. This offset frequency can be accurately determined by measuring the atomic vibrational frequencies in the lattice.[76]

3.5 Atomic elements applicable to optical lattice clocks

The optical lattice clock scheme is generally applicable to atoms in groups II and IIb[77] such as Ca,[78] Yb,[79] Zn, Cd,[80] and Hg[16] that have hyperfine-mixed $J = 0 \rightarrow J = 0$ transition between long-lived states. Alternatively, a multiphoton excitation of the clock transition,[81,82] or the mixing of the $^3P_0$ state with the $^3P_1$ state using a magnetic field[63] or an elliptically polarized light[83] may allow the use of even isotopes that exhibit purely scalar nature of the $J = 0$ state. The optical lattice clock with the best performance needs to be experimentally explored among possible candidates because of difficulties in predicting some of the uncertainties associated with higher-order light field perturbations; such as resonant contribution to the 4th-order light shifts and multiphoton ionization processes.

Potential high precision and wide applicability of the optical lattice clock scheme to other atom species would enable the exploration of a possible variation in fine structure constant.[84] Thus far, frequencies of several atom clocks operated at the 10^{-15} level have been compared over a few years to verify the constancy of $|\dot{\alpha}/\alpha|$ at the level of $(-1.6 \pm 2.3) \times 10^{-17}$/yr.[7] Assuming $\Delta\alpha/\alpha = 10^{-16}$, at which level per year astrophysical determinations have given controversial results,[84] the fractional change in the clock frequency[85] $\delta\nu/\nu_0$ can be 6.2×10^{-18}, 3.1×10^{-17}, and 8.1×10^{-17} for Sr-, Yb-, and Hg-based optical lattice clocks, respectively. Heavier atoms such as Yb and Hg tend to show higher sensitivity as relativistic correction is proportional to the squared atomic number Z^2. One may take a Sr lattice clock as an anchor to detect the fractional frequency change of the Hg lattice clock at the $\delta\nu/\nu_0 = 10^{-17}$ level, which can be accurately measured with an optical frequency comb technique.

4. Experimental Realization of an Optical Lattice Clock with ^{87}Sr

4.1 Spectroscopy of the $^1S_0$–$^3P_0$ clock transition of ^{87}Sr in an optical lattice

The ultranarrow $^1S_0(F = 9/2)$–$^3P_0(F = 9/2)$ clock transition of ^{87}Sr with a natural linewidth of 1 mHz was first observed in 2003 by two groups simultaneously. The Paris group[86] investigated the transition by saturated absorption spectroscopy in free space to determine its transition frequency with 11 digits, while the Tokyo[9] group observed the transition with a linewidth of 700 Hz in an optical lattice tuned to the magic wavelength, thus opening up a new era for optical lattice clocks. Figure 6 shows the experimental setup used in the early stages of the lattice clock experiments.[9,10] ^{87}Sr atoms were laser-cooled and trapped on the $^1S_0$–$^3P_0$ transition by the dynamic magneto-optical trapping (DMOT) technique.[87] Roughly 10^4 atoms with a temperature of about 2 μK were loaded into a 20-μK-deep 1D optical lattice that was formed by the standing wave of a lattice laser, providing atoms with Lamb–Dicke confinement along the axial direction. In this experiment,[9] magic wavelength was determined to be 813.5(9) nm by investigating the narrowing of the clock spectra as a result of the cancellation of the light shift [see Fig. 7(a)]. At this magic wavelength, the observed clock spectrum is shown in Fig. 7(b), which consisted of heating and cooling sidebands at ≈±64 kHz, and a narrow carrier of 700 Hz (see inset). Afterwards, the π-pulse excitation of the clock transition by a tightly stabilized clock laser to a high-finesse ULE cavity reduced the linewidth to about 20 Hz in 2004.[10] Presently, the Fourier-limited linewidth of a few Hz is routinely obtained for optical lattice clocks across the world.

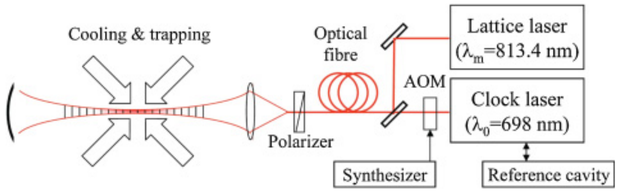

Fig. 6. (Color online) Schematic diagram of the experimental setup for Sr spectroscopy used in the early experiments.[9,10] Ultracold ^{87}Sr atoms are loaded into a 1D optical lattice produced by the standing wave of a Ti-sapphire laser tuned to the magic wavelength. The atoms are confined at the antinodes of a standing wave, which give subwavelength confinement along the axial direction. The atoms interact with the clock laser propagating along this axis and the Lamb–Dicke condition is satisfied. AOM, acousto-optic modulator.

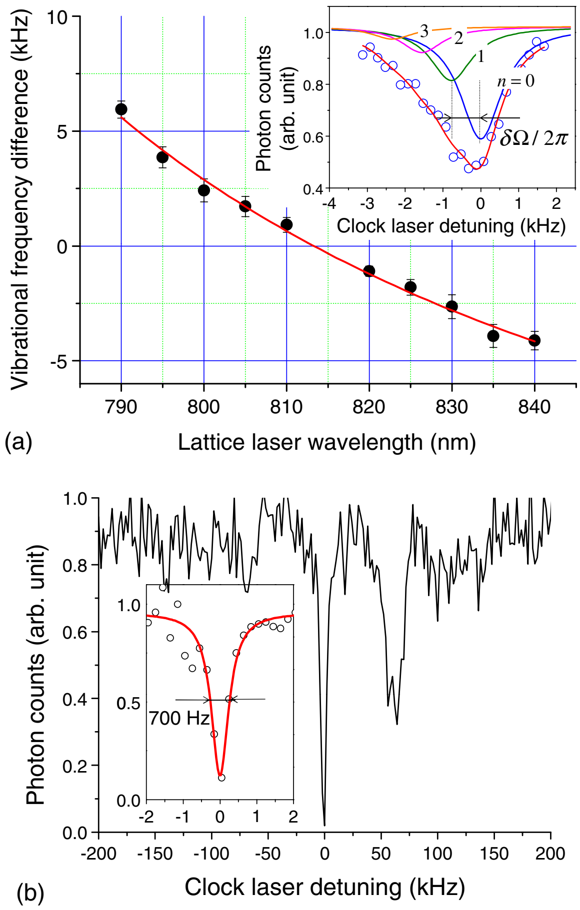

Fig. 7. (Color online) (a) The first determination of magic wavelength was performed by measuring the spectral line broadening, as shown in the inset. This broadening is used to reveal the vibrational frequency differences in two states of the clock transition, which is plotted as a function of lattice laser wavelength to determine the degenerate wavelength to be $\lambda_L = 813.5 \pm 0.9$ nm. (b) The first clock transition was measured in the "magic lattice" in 2003. The upper and the lower sidebands at ≈±64 kHz correspond to the heating and the cooling sidebands, respectively. The inset shows the recoilless spectrum (the carrier component) with a linewidth of 0.7 kHz (FWHM).

4.2 Frequency stabilization of the clock laser to the atomic transition

4.2.1 Normalization of the clock spectrum

The frequency stabilization of the clock laser to the spectrum center was realized by the feedback control of AOM frequency (see Fig. 8) using the error signal $f_{\rm err}(t_n)$ obtained by a digital servo loop as

$$f_{\rm err}(t_{n+1}) = f_{\rm err}(t_n) + \delta f(t_n), \tag{4}$$

where $\delta f(t_n)$ is the correction signal measured in the n-th interrogation period at $t = t_n$ as

$$\delta f \approx \gamma \times \frac{\kappa(+\gamma/2) - \kappa(-\gamma/2)}{2}, \tag{5}$$

where γ is the full width at half maximum (FWHM) linewidth of the observed spectrum, and $\kappa(\pm\gamma/2)$ is the atom excitation probability near the side slopes of the Rabi excitation spectrum with respect to the stabilized line center at $t = t_n$.

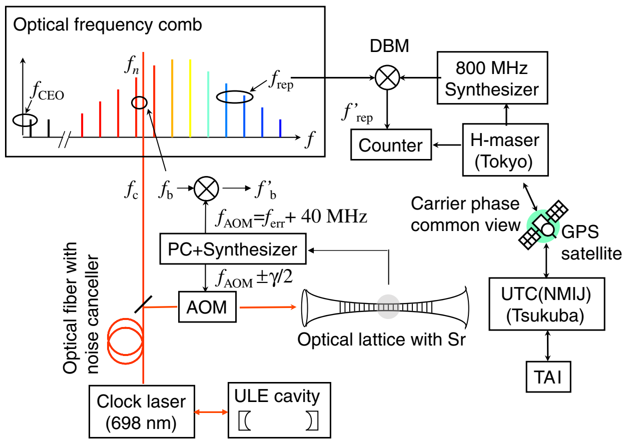

Fig. 8. (Color online) Schematic diagram of the experimental setup. AOM, acousto-optic modulator; PC, personal computer; DBM, double-balanced mixer; ULE, ultralow expansion; GPS, global positioning system; UTC, coordinated universal time; NMIJ, National Metrology Institute of Japan; TAI, international atomic time. A beat signal $f'_{\rm b}$ was used to stabilize the n-th comb component to the Sr transition frequency.

To remove the atom number fluctuation in measuring excitation probability, the normalization of the atom number was carried out by measuring the atom populations of $N_{\rm S}$ and $N_{\rm P}$ of the $^1{\rm S}_0$–$^3{\rm P}_0$ clock transition.[23] The excited atom fraction κ was thus derived as, $\kappa = N_{\rm P}/(N_{\rm S}+N_{\rm P})$, which was measured as a function of the detuning Δ of the clock laser frequency, i.e., $\kappa(\Delta)$.

4.2.2 Spin polarization and vector light shift cancellation

To suppress the collision shift as well as to remove the vector light shift arising from the elliptical polarization of the lattice laser, we have implemented the spin polarization of fermionic atoms before interrogating clock transition.[23] The spin polarization was performed by shining circular polarized resonant light on the $^1{\rm S}_0(F=9/2)$–$^3{\rm P}_1(F=9/2)$ transition at 689 nm (see Fig. 3). The differential g-factor in the clock transition introduces a first-order Zeeman shift of $m_{\rm F}\times 106\,{\rm Hz/G}$[18] for the π-transition excited at the $m_{\rm F}$ sublevel in the $^1{\rm S}_0(F=9/2)$ ground state. This first-order Zeeman shift as well as the vector light shift can be eliminated by averaging the two transition frequencies $f_\pm$ corresponding to the $^1{\rm S}_0(F=9/2, m_{\rm F}=\pm 9/2)$–$^3{\rm P}_0(F=9/2, m_{\rm F}=\pm 9/2)$ transition. Transition frequency is therefore given by

$$f_0 = \frac{f_+ + f_-}{2}. \qquad (6)$$

This technique has been routinely applied to later experiments.[88,89)]

Since a single measurement took 1 s or less, a cycle time $t_{\rm c} = t_n - t_{n-1}$ of nearly 2 s was required to determine one of the Zeeman components, $f_\pm$. The cycle time required for cooling, trapping, and interrogating atoms in the lattice was not optimized in this experiment. Further reduction in cycle time to less than 1 s will be feasible in a future experiment.

4.3 Absolute frequency measurement of the ^{87}Sr optical lattice clock

The absolute frequency measurement of an optical clock is rather straightforward if a primary time standard is located at the same site as the optical clock.[11] If this is not the case, a precise frequency link is necessary between the optical clock and the primary time standard. We established a GPS frequency link in 2006[23] and a coherent optical fiber link in 2008[59,60] for the frequency measurement of the ^{87}Sr optical lattice clock at the University of Tokyo based on time standards located 51 km away from Tokyo at the National Metrology Institute of Japan. The Boulder group[17] has introduced an optical fiber link between kilometer-distant JILA and NIST for the frequency measurement of the ^{87}Sr optical lattice clock.

4.3.1 Frequency measurement using a GPS frequency link

Figure 8 shows a schematic of the experiment for frequency measurement using a GPS frequency link. In this experimental configuration, since the laser light after the AOM was a pulsed-light used for Sr spectroscopy, its frequency could not be directly measured with the frequency comb. We first measured the beat frequency $f_{\rm b} = |f_{\rm c} - f_n|$ between the clock laser $f_{\rm c}$ and the n-th tooth of the comb f_n with a photodiode. We then electronically mixed the beat note $f_{\rm b}$ with $f_{\rm AOM} = f_{\rm err} + 40\,{\rm MHz}$ with a double-balanced mixer (DBM) and extracted the frequency component

$$f'_{\rm b} = |f_{\rm c} + f_{\rm AOM} - f_n|, \qquad (7)$$

which corresponded to the +1-order light diffracted by the AOM. This frequency is equal to the beat frequency between the Sr-transition frequency $f_{\rm Sr} = f_{\rm c} + f_{\rm AOM}$ and the n-th tooth of the comb f_n. In our measurement scheme, $f'_{\rm b}$ was used to phase-lock the n-th comb component to the Sr clock transition by feedback controlling the cavity length of the mode-locked laser. In this way, the entire comb was locked to the Sr clock transition, which means that the stability of each comb component and the repetition rate of the comb ($f_{\rm rep}$) follow that of the Sr clock transition. $f_{\rm rep}$ was measured against the H-maser.

To calibrate the frequency of the H-maser, GPS carrier phase receivers were employed at both sites, the University of Tokyo and NMIJ. The H-maser was calibrated on the basis of the Coordinated Universal Time of NMIJ [UTC(NMIJ)] using the GPS carrier-phase technique with the analysis software "GIPSY".[22] The relationship between the UTC(NMIJ) and the International Atomic Time (TAI) can be found in the monthly reports of the Circular-T of the Bureau International des Poids et Mesures (BIPM).[90]

Figure 9 shows the measured frequency of the Sr lattice clock. The absolute frequency of the Tokyo Sr lattice clock was determined to be 429,228,004,229,875(4) Hz using the GPS frequency link. The main contribution of the measurement uncertainty was the uncertainty of the GPS link. In addition to the Tokyo–NMIJ result, we also show the results from the JILA[12] and the SYRTE[11] groups available in 2006. The weighted average of the frequencies measured by the three groups gives an average frequency of 429,228,004,229,876.6 Hz, which is within the error bars of the three groups. The standard deviation of the mean is 3.2 Hz. There is good agreement between the measurement results of the three groups. These results were reported to the CIPM for making a decision of the adoption of the Sr lattice clock as one of the "secondary representations

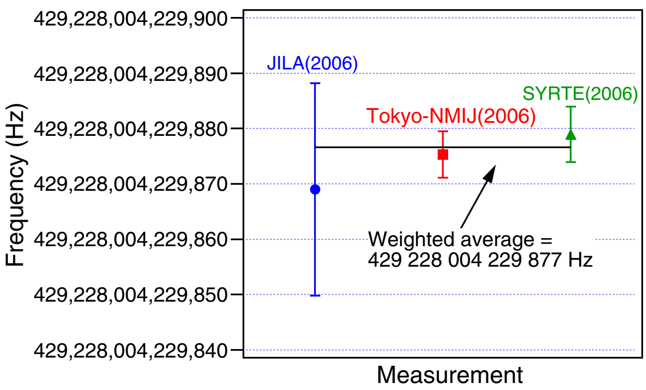

Fig. 9. (Color online) Comparison of the absolute frequencies of the Sr lattice clock measured by the Tokyo–NMIJ,[23] JILA,[12] and SYRTE[11] groups, which were available on the occasion of the CIPM meeting held in October 2006.

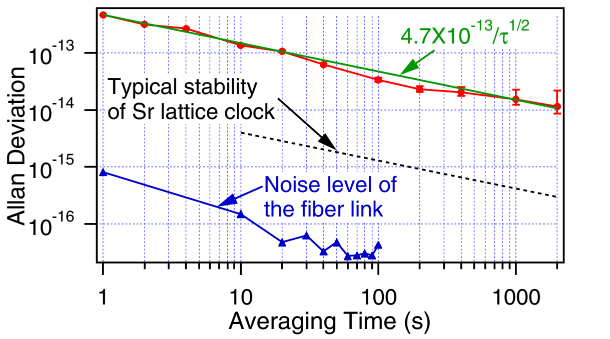

Fig. 11. (Color online) Allan deviation of the measured Sr frequency (solid curve with filled circles) based on a fiber-linked H-maser.[60] The Allan deviation is given by $4.7 \times 10^{-13}/\tau^{1/2}$ (solid line), where the $1/\tau^{1/2}$ slope indicates white frequency noise. Also shown are the Allan deviations of the Sr optical lattice clock (dotted line)[72] and the fiber link (solid curve with open circles).[59]

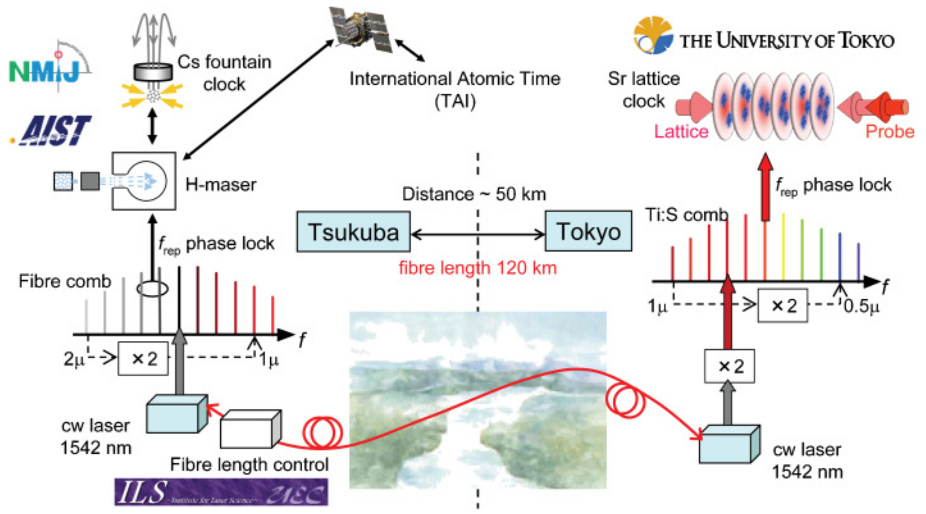

Fig. 10. (Color online) Diagram of remote absolute frequency measurement using a fiber link between two cities (Tokyo and Tsukuba) in Japan. The University of Tokyo and the National Metrology Institute of Japan, which are about 50 km apart, are linked by a 120-km-long fiber. A Sr optical lattice clock is operated in Tokyo, while a Cs fountain clock and a link to TAI are established in Tsukuba.

of the second" (see also §6). This is an important step in the research on an "optical lattice clock" in terms of the redefinition of the second.

4.3.2 Frequency measurement using a 120 km coherent optical fiber transfer

To further reduce the measurement uncertainty of the Sr lattice clock, we have introduced a 120-km-long optical fiber link between the University of Tokyo and the NMIJ at Tsukuba.[60] Figure 10 shows a diagram of a remote absolute frequency measurement using the intercity optical carrier fiber link. In the outline, the Sr lattice clock located in Tokyo was measured on the basis of an H-maser in Tsukuba using a fiber link, while the H-maser was calibrated using a Cs fountain clock and a frequency link to TAI.

A fiber comb[31] was phase-locked to the H-maser. A narrow linewidth fiber DFB laser operating at 1542 nm was phase-locked to the fiber comb to convert the microwave signal of the H-maser into an optical signal for fiber transfer. The input optical power at Tsukuba was about 10 mW, which is limited by stimulated Brillouin scattering. Consequently the output power at Tokyo was about 50 nW. An external cavity diode laser located in Tokyo was used as a repeater. The laser was phase-locked to the transferred light with an offset frequency to distinguish the round-trip light from the stray reflections in the fiber. The light was then sent back to Tsukuba so that its phase could be compared with that of the original light, thus allowing the detection of the fiber length fluctuation[55] caused by both acoustic noise and temperature variations. A fiber stretcher was used to servo-control fiber length and thus suppress the phase noise, while an acousto-optic modulator (AOM) was used to expand the dynamic range of the fiber stretcher.[59] The phase noise suppression can also be realized using only the AOM transducer. The frequency of the repeater laser in Tokyo was doubled using a periodically poled lithium niobate (PPLN) crystal, and was measured using a Ti:S comb at 771 nm. The Ti:S comb phase-locked to the Sr lattice clock converted the Sr frequency to the entire Ti:S comb measurement range covering 500 to 1100 nm.

Figure 11 shows the Allan deviation of the measured Sr frequency based on the fiber-linked H-maser. The Allan deviation was given by $4.7 \times 10^{-13}/\tau^{1/2}$ (solid line), where the $1/\tau^{1/2}$ slope indicates white frequency noise. The Allan

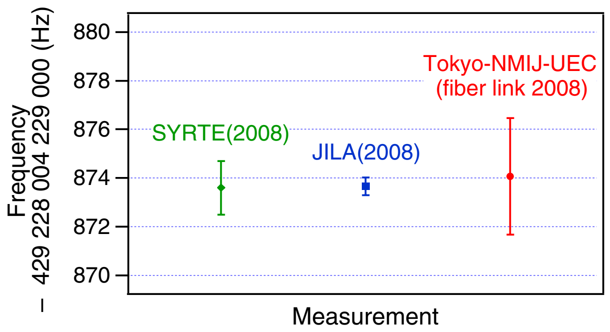

Fig. 12. (Color online) Comparison of the absolute frequencies of Sr lattice clocks measured by three groups. The absolute frequency of the Sr lattice clock in Tokyo is 429228004229874.1(2.4) Hz,[60] which agrees with the results from JILA[17] and SYRTE[89] with a fractional uncertainty of 6×10^{-16}.

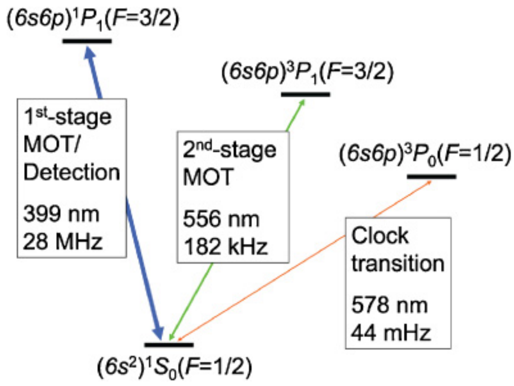

Fig. 13. (Color online) Energy levels of ^{171}Yb. Wavelengths and natural linewidths are indicated for the relevant cooling, trapping, and clock transitions.

deviation at 1 s was mainly limited by the stability of the H-maser. The typical Allan deviation of the Sr lattice clock is also shown in Fig. 11 as a dotted line ($1 \times 10^{-14}/\tau^{1/2}$ for an averaging time > 100 s),[72] and was about 30 times smaller than that of the measured frequency noise. The frequency stability of the coherent optical carrier transfer with active phase noise cancellation was 8×10^{-16} at 1 s[59] and is shown as a solid curve with open circles in Fig. 11. This result indicates that the clock's performance was transferred without degrading its stability.

Figure 12 shows a comparison of the absolute frequencies of the Sr lattice clock measured by the three groups in 2008. The absolute frequency of the Tokyo Sr lattice clock was determined to be 429,228,004,229,874.1(2.4) Hz using the 120-km fiber link. The center value of our newly determined Sr frequency agrees with the center values of the JILA[17] and SYRTE[89] results with a standard deviation of 0.27 Hz (corresponding to a fractional uncertainty of 6×10^{-16}). The measured frequency of the Sr optical lattice clock was reported to the CIPM for updating the frequency of "the secondary representations of the second".

5. ^{171}Yb Optical Lattice Clocks

Yb has two stable odd isotopes, ^{171}Yb and ^{173}Yb, which also appear to be excellent candidate optical frequency standards with the lattice clock scheme.[79] The absolute frequency of the $^1S_0$–$^3P_0$ clock transition in ^{171}Yb and ^{173}Yb was measured for an atomic cloud released from a magneto-optical trap (MOT) with an uncertainty of 4.4 kHz.[91] On the other hand, an optical lattice clock has also been realized with the even isotope ^{174}Yb by introducing a static magnetic field to induce a nonzero dipole transition probability for the forbidden clock transition.[65] The absolute frequency of the clock transition of bosonic ^{174}Yb atoms in an optical lattice has been determined with an uncertainty of 0.8 Hz.[92] The optical-lattice-induced hyperpolarizability frequency shift uncertainty was measured at less than 7×10^{-17} of the clock frequency (applicable to any Yb isotope),[93] indicating that the Yb optical lattice clock is a promising candidate as a next-generation optical frequency standard.

^{171}Yb has attracted considerable attention because it has a reasonable natural abundance of 14% and a relatively simple $I = 1/2$ spin system, which means we could avoid the need for an extra optical pumping process in the experiment. Figure 13 shows the relevant energy level diagram of ^{171}Yb. The $^1S_0$–$^3P_0$ transition has a natural linewidth of 44 mHz and is used as a clock transition. The clock laser at 578 nm can be generated using the sum-frequency generation of a 1319-nm Nd:YAG laser and a 1030-nm Yb:YAG or Yb fiber laser with a PPLN waveguide device.[94] ^{171}Yb can be trapped and cooled by using two stages of MOT. The first-stage MOT uses a strong dipole-allowed transition ($^1S_0$–$^3P_0$; 399 nm, natural linewidth of 28 MHz), while the second-stage MOT uses the spin-forbidden transition ($^1S_0$–$^3P_1$; 556 nm, natural linewidth of 182 kHz).

The absolute frequency of the ^{171}Yb lattice clock at the NMIJ was measured to be 518,295,836,590,864(28) Hz in 2009.[13] The determined magic wavelength was 759.353(3) nm. The uncertainty of the absolute frequency was mainly contributed by the frequency scan step in spectroscopy and can be reduced by locking the clock laser to the observed spectrum. The measurement results were reported to the CIPM in June 2009 for a discussion of new frequency standards. Our measured frequency agrees well with the value of 518,295,836,590,865.2(7) Hz, recently reported from the National Institute of Standards and Technology (NIST).[14]

6. "Secondary Representations of the Second"

The rapid development of optical clocks has led to a situation in which the accuracy of optical clocks is limited by the Cs microwave standard. This means that even if we can show that the reproducibility of an optical clock is better than that of the Cs clock, we are not able to demonstrate better accuracy of the formor than of the latter. In 2001, the Consultative Committee for Time and Frequency (CCTF), as one of the consultative committees under the CIPM, set up a working group to establish a frequency list called the "Secondary Representations of the Second". With the Secondary Representations of the Second, we can realize the "second" with either a microwave or an optical frequency. This would help with the detailed evaluation of reproducibility at the highest level, and significantly aid the process of comparing different standards in the preparation of a future redefinition.

As candidates for the redefinition of the second, the criteria for the adoption of a secondary representation of the second are as follows:

Table I. Secondary representations of the second.

	Reference transition	Frequency (Hz)	Uncertainty
Microwave	^{87}Rb, ground-state hyperfine	6834682610.904324	3×10^{-15}
Optical	$^{88}Sr^{+}$, 5s $^{2}S_{1/2}$–4d $^{2}D_{5/2}$	444779044095484	7×10^{-15}
Optical	$^{199}Hg^{+}$, 5d^{10}6s $^{2}S_{1/2}(F=0)$–5d $^{2}D_{5/2}(F=2)$	1064721609899145	3×10^{-15}
Optical	$^{171}Yb^{+}$, 6s $^{2}S_{1/2}(F=0)$–5d $^{2}D_{3/2}(F=2)$	688358979309308	9×10^{-15}
Optical	^{87}Sr, 5s^{2} $^{1}S_{0}$–5s 5p $^{3}P_{0}$	429228004229873.7	1×10^{-15}

1) The unperturbed frequency of a quantum transition suitable as a secondary representation of the second must have an uncertainty that is evaluated and documented so as to meet the requirements adopted for the primary frequency standard for use in International Atomic Time.
2) This uncertainty should be no larger than about a factor of 10 of the primary standards of that date that serve as the best realizations of the second.

Detailed description on the secondary representations of the second can be found elsewhere.[95]

In 2006, the CIPM recommended one microwave and three optical frequency standards as the secondary representations of the second based on the recommendations from the CCTF (listed in Table I). The microwave secondary representation is on the basis of the hyperfine transition of the ground state of ^{87}Rb. The optical secondary representations are based on optical transitions of $^{88}Sr^{+}$, $^{199}Hg^{+}$, $^{171}Yb^{+}$, and ^{87}Sr. The ^{87}Sr recommendation of 2006 was decided on the basis of the measurement results of the Sr lattice clock up to 2006.[11,12,23] At the CCTF 2009, the frequency value and uncertainty of ^{87}Sr were updated using new measurement results of the Sr lattice clock up to 2009.[17,60,89] Up to now, ^{87}Sr has had the lowest uncertainty (1×10^{-15}) among all the secondary representations. In addition, ^{171}Yb also became a recommended frequency standard in 2009 on the basis of the measurement result at NMIJ,[13] and is to be further studied to be recommended as a secondary representation of the second.

7. Outlook

It is now an exciting period for researchers working on optical frequency metrology. Research activities related to optical clocks, frequency combs, and optical frequency transfer have been developing rapidly. The secondary representations of the second will be updated frequently. One of these standards may lead to a new definition of the second. Works toward a new definition are to be discussed in detail at the CCTF meeting. We need to consider the next issues.

1) The uncertainty evaluation of optical clocks is important. As a new definition of the second, an optical clock must have a smaller uncertainty than the Cs clock. Since the uncertainty evaluation of an optical clock based on the Cs clock will be limited by the Cs clock, an uncertainty evaluation by comparing two optical clocks is necessary. The uncertainties of the $^{199}Hg^{+}$ and $^{27}Al^{+}$ optical standards have recently been reported to be 1.9×10^{-17} and 2.3×10^{-17}, respectively, by comparing the two optical standards.[7] The reported uncertainties are about one order of magnitude smaller than that of the Cs clock.
2) It is better if multiple national institutes work on the same type of clock. This is important for the confirmation of the equality of the standards and also the reliability. Currently, a large number of researchers believe in the bright future of the optical lattice clock and a number of national institutes are investing their research resources into optical lattice clocks.
3) We need to consider the contribution of the secondary representations to the TAI. This will be a report to BIPM detailing the experimental results obtained in a particular reporting period including uncertainty budget and references.

To further improve the stability of the optical lattice clock, it is important to realize an ultrastable laser for the clock transition. The advantage of the lattice clock over the single-ion clock is its high signal-to-noise (S/N) due to the contribution of a large number of atoms in the lattice clock. However, if the clock laser is not sufficiently stable in the short term (say at 1 s), the inherently high S/N in the lattice clock cannot be fully utilized. Recently, a short-term stability of 5.6×10^{-16} at 1 s has been realized for a vibration-insensitive cavity.[96] The idea of reduction in sensitivity to thermal noise is proposed for the realization of an ultrastable laser.[97]

Remote comparison of optical clocks in different institutes is becoming an important issue for the development of optical clocks. This can be realized using optical coherent transfer with optical fiber networks, because the stability of optical carrier transfer is better than the stability of optical clocks.[24,25,59] In Japan, there are three laboratories working on optical clocks: the University of Tokyo, working on Sr, Yb, and Hg lattice clocks; the NMIJ, working on Yb and Sr lattice clocks; and the National Institute of Information and Communications Technology (NICT), working on Sr lattice clock and Ca^{+} clocks. They are located within an area with a diameter of 80 km. The fiber network between the three institutes should lead to a precise comparison of various optical clocks at levels of 10^{-17} to 10^{-18}. In Germany, a 900-km-long fiber link has been established for transferring optical frequencies and connecting atomic clocks between several national institutes.[98] The ability to compare distant optical clocks through optical fiber links without any degradation in accuracy or stability should promote research on tests designed to determine possible violations of the equivalence principle of general relativity and on the possible time variation of the fine structure constant.[85] Furthermore, the ability to compare distant optical clocks at the highest possible level of accuracy is also important for a possible redefinition of the second based on an optical clock.

Acknowledgments

The authors thank Dr. M. Takamoto and Dr. T. Akatsuka of the University of Tokyo for their contributions to the Sr lattice clock experiment; Dr. M. Imae, Y. Fujii, Dr. Amemiya, Dr. S. Yanagimachi, Dr. A. Takamizawa, Dr. K. Watabe, and Dr. T. Ikegami of the National Metrology Institute of Japan for their contributions in the time keeping and transfer experiment; Dr. M. Musha, Professor K. Nakagawa, and Professor K. Ueda of the University of Electro-Communications for their contributions in the fiber link experiment; Dr. T. Kohno, M. Yasuda, K. Hosaka, H. Inaba, and Y. Nakajima from the National Metrology Institute of Japan for their contributions in the Yb lattice clock experiment. This research was partially supported by the Photon Frontier Network Program of the Ministry of Education, Culture, Sports, Science and Technology, Japan.

1) L. Essen and J. V. L. Parry: Philos. Trans. R. Soc., Ser. A **250** (1957) 45.
2) T. P. Heavner, S. R. Jefferts, E. A. Donley, J. H. Shirley, and T. E. Parker: Metrologia **42** (2005) 411.
3) Th. Udem, J. Reichert, R. Holzwarth, and T. W. Hänsch: Phys. Rev. Lett. **82** (1999) 3568.
4) S. A. Diddams, D. J. Jones, J. Ye, S. T. Cundiff, J. L. Hall, J. K. Ranka, R. S. Windeler, R. Holzwarth, Th. Udem, and T. W. Hänsch: Phys. Rev. Lett. **84** (2000) 5102.
5) D. J. Jones, S. A. Diddams, J. K. Ranka, A. Stentz, R. S. Windeler, J. L. Hall, and S. T. Cundiff: Science **288** (2000) 635.
6) H. G. Dehmelt: IEEE Trans. Instrum. Meas. **31** (1982) 83.
7) T. Rosenband, D. B. Hume, P. O. Schmidt, C. W. Chou, A. Brusch, L. Lorini, W. H. Oskay, R. E. Drullinger, T. M. Fortier, J. E. Stalnaker, S. A. Diddams, W. C. Swann, N. R. Newbury, W. M. Itano, D. J. Wineland, and J. C. Bergquist: Science **319** (2008) 1808.
8) H. Katori: in *Proc. 6th Symp. Frequency Standards and Metrology*, ed. P. Gill (World Scientific, Singapore, 2002) p. 323.
9) M. Takamoto and H. Katori: Phys. Rev. Lett. **91** (2003) 223001.
10) M. Takamoto, F.-L. Hong, R. Higashi, and H. Katori: Nature **435** (2005) 321.
11) R. Le Targat, X. Baillard, M. Fouche, A. Brusch, O. Tcherbakoff, G. D. Rovera, and P. Lemonde: Phys. Rev. Lett. **97** (2006) 130801.
12) A. D. Ludlow, M. M. Boyd, T. Zelevinsky, S. M. Foreman, S. Blatt, M. Notcutt, T. Ido, and J. Ye: Phys. Rev. Lett. **96** (2006) 033003.
13) T. Kohno, M. Yasuda, K. Hosaka, H. Inaba, Y. Nakajima, and F.-L. Hong: Appl. Phys. Express **2** (2009) 072501.
14) N. D. Lemke, A. D. Ludlow, Z. W. Barber, T. M. Fortier, S. A. Diddams, Y. Jiang, S. R. Jefferts, T. P. Heavner, T. E. Parker, and C. W. Oates: Phys. Rev. Lett. **103** (2009) 063001.
15) M. Petersen, R. Chicireanu, S. T. Dawkins, D. V. Magalhães, C. Mandache, Y. Le Coq, A. Clairon, and S. Bize: Phys. Rev. Lett. **101** (2008) 183004.
16) H. Hachisu, K. Miyagishi, S. G. Porsev, A. Derevianko, V. D. Ovsiannikov, V. G. Pal'chikov, M. Takamoto, and H. Katori: Phys. Rev. Lett. **100** (2008) 053001.
17) G. K. Campbell, A. D. Ludlow, S. Blatt, J. W. Thomsen, M. J. Martin, M. H. G. de Miranda, T. Zelevinsky, M. M. Boyd, J. Ye, S. A. Diddams, T. P. Heavner, T. E. Parker, and S. R. Jefferts: Metrologia **45** (2008) 539.
18) H. Katori, M. Takamoto, V. G. Pal'chikov, and V. D. Ovsiannikov: Phys. Rev. Lett. **91** (2003) 173005.
19) A. Bartels, S. A. Diddams, C. W. Oates, G. Wilpers, J. C. Bergquist, W. H. Oskay, and L. Hollberg: Opt. Lett. **30** (2005) 667.
20) J. Millo, R. Boudot, M. Lours, P. Y. Bourgeois, A. N. Luiten, Y. Le Coq, Y. Kersale, and G. Santarelli: Opt. Lett. **34** (2009) 3707.
21) L.-S. Ma, Z. Bi, A. Bartels, L. Robertosson, M. Zucco, R. Windeler, G. Wilpers, C. Oates, L. Hollberg, and S. A. Diddams: Science **303** (2004) 1843.
22) K. M. Larson and J. Levine: IEEE Trans. Ultrason. Ferroelectr. Freq. Control **46** (1999) 1001.
23) M. Takamoto, F.-L. Hong, R. Higashi, Y. Fujii, M. Imae, and H. Katori: J. Phys. Soc. Jpn. **75** (2006) 104302.
24) S. M. Foreman, A. D. Ludlow, M. H. G. de Miranda, J. E. Stalnaker, S. A. Diddams, and J. Ye: Phys. Rev. Lett. **99** (2007) 153601.
25) N. R. Newbury, P. A. Williams, and W. C. Swann: Opt. Lett. **32** (2007) 3056.
26) J. C. Knight, T. A. Birks, P. St. J. Russell, and D. M. Atkin: Opt. Lett. **21** (1996) 1547.
27) J. K. Ranka, R. S. Windeler, and A. J. Stentz: Opt. Lett. **25** (2000) 796.
28) F.-L. Hong, K. Minoshima, A. Onae, H. Inaba, H. Takada, A. Hirai, H. Matsumoto, T. Sugiura, and M. Yoshida: Opt. Lett. **28** (2003) 1516.
29) B. R. Washburn, S. A. Diddams, N. R. Newbury, J. W. Nicholson, M. F. Yan, and C. G. Jorgensen: Opt. Lett. **29** (2004) 250.
30) T. R. Schibli, K. Minoshima, F.-L. Hong, H. Inaba, A. Onae, H. Matsumoto, I. Hartl, and M. E. Fermann: Opt. Lett. **29** (2004) 2467.
31) H. Inaba, Y. Daimon, F.-L. Hong, A. Onae, K. Minoshima, T. R. Schibli, H. Matsumoto, M. Hirano, T. Okuno, M. Onishi, and M. Nakazawa: Opt. Express **14** (2006) 5223.
32) W. C. Swann, J. J. McFerran, I. Coddington, N. R. Newbury, I. Hartl, M. E. Fermann, P. S. Westbrook, J. W. Nicholson, K. S. Feder, C. Langrock, and M. M. Fejer: Opt. Lett. **31** (2006) 3046.
33) N. R. Newbury and W. C. Swann: J. Opt. Soc. Am. B **24** (2007) 1756.
34) Y. Nakajima, H. Inaba, K. Hosaka, K. Minoshima, A. Onae, M. Yasuda, T. Kohno, S. Kawato, T. Kobayashi, T. Katsuyama, and F.-L. Hong: Opt. Express **18** (2010) 1667.
35) A. Winter, F. Ö. Ildayc, O. D. Mücke, R. Ell, H. Schlarb, P. Schmüser, and F. X. Kärtner: Nucl. Instrum. Methods Phys. Res., Sect. A **557** (2006) 299.
36) C. Gohle, Th. Udem, M. Herrmann, J. Rauschenberger, R. Holzwarth, H. A. Schuessler, F. Krausz, and T. W. Hänsch: Nature **436** (2005) 234.
37) R. J. Jones, K. D. Moll, M. J. Thorpe, and J. Ye: Phys. Rev. Lett. **94** (2005) 193201.
38) M. Zimmermann, Ch. Gohle, R. Holzwarth, Th. Udem, and T. W. Hänsch: Opt. Lett. **29** (2004) 310.
39) O. D. Mucke, O. Kuzucu, F. N. C. Wong, E. P. Ippen, F. X. Kaertner, S. M. Foreman, D. J. Jones, L.-S. Ma, J. L. Hall, and J. Ye: Opt. Lett. **29** (2004) 2806.
40) J. Jiang, A. Onae, H. Matsumoto, and F.-L. Hong: Opt. Express **13** (2005) 1958.
41) P. Malara, P. Maddaloni, G. Gagliardi, and P. De Natale: Opt. Express **16** (2008) 8242.
42) K. Takahata, T. Kobayashi, H. Sasada, Y. Nakajima, H. Inaba, and F.-L. Hong: Phys. Rev. A **80** (2009) 032518.
43) M. J. Thorpe, D. Balslev-Clausen, M. S. Kirchner, and J. Ye: Opt. Express **16** (2008) 2387.
44) T. Steinmetz, T. Wilken, C. Araujo-Hauck, R. Holzwarth, T. W. Hänsch, L. Pasquini, A. Manescau, S. D'Odorico, M. T. Murphy, T. Kentischer, W. Schmidt, and Th. Udem: Science **321** (2008) 1335.
45) T. J. Quinn: Metrologia **40** (2003) 103.
46) R. Felder: Metrologia **42** (2005) 323.
47) C. W. Oates, E. A. Curtis, and L. Hollberg: Opt. Lett. **25** (2000) 1603.
48) G. Wilpers, T. Binnewies, C. Degenhardt, U. Sterr, J. Helmcke, and F. Riehle: Phys. Rev. Lett. **89** (2002) 230801.
49) R. H. Dicke: Phys. Rev. **89** (1953) 472.
50) C. Degenhardt, H. Stoehr, C. Lisdat, G. Wilpers, H. Schnatz, B. Lipphardt, T. Nazarova, P. Pottie, U. Sterr, and J. Helmcke: Phys. Rev. A **72** (2005) 62111.
51) J. E. Stalnaker, S. A. Diddams, T. M. Fortier, K. Kim, L. Hollberg, J. C. Bergquist, W. M. Itano, M. J. Delany, L. Lorini, W. H. Oskay, T. P. Heavner, S. R. Jefferts, F. Levi, T. E. Parker, and J. Shirley: Appl. Phys. B **89** (2007) 167.
52) H. S. Margolis, G. P. Barwood, G. Huang, H. A. Klein, S. N. Lea, K. Szymaniec, and P. Gill: Science **306** (2004) 1355.
53) Chr. Tamm, S. Weyers, B. Lipphardt, and E. Peik: Phys. Rev. A **80** (2009) 043403.
54) C.-W. Chou, D. B. Hume, J. C. J. Koelemeij, D. J. Wineland, and T. Rosenband: Phys. Rev. Lett. **104** (2010) 070802.
55) L.-S. Ma, P. Jungner, J. Ye, and J. L. Hall: Opt. Lett. **19** (1994) 1777.
56) J. Ye, J. L. Peng, R. J. Jones, K. W. Holman, J. L. Hall, D. J. Jones, S. A. Diddams, J. Kitching, S. Bize, J. C. Bergquist, L. W. Hollberg, L. Robertsson, and L. S. Ma: J. Opt. Soc. Am. B **20** (2003) 1459.
57) O. Lopez, A. Amy-Klein, C. Daussy, C. Chardonnet, F. Narbonneau, M. Lours, and G. Santarelli: Eur. Phys. J. D **48** (2008) 35.

58) A. D. Ludlow, T. Zelevinsky, G. K. Campbell, S. Blatt, M. M. Boyd, M. H. G. de Miranda, M. J. Martin, J. W. Thomsen, S. M. Foreman, J. Ye, T. M. Fortier, J. E. Stalnaker, S. A. Diddams, Y. Le Coq, Z. W. Barber, N. Poli, N. D. Lemke, K. M. Beck, and C. W. Oates: Science **319** (2008) 1805.
59) M. Musha, F.-L. Hong, K. Nakagawa, and K. Ueda: Opt. Express **16** (2008) 16459.
60) F.-L. Hong, M. Musha, M. Takamoto, H. Inaba, S. Yanagimachi, A. Takamizawa, K. Watabe, T. Ikegami, M. Imae, Y. Fujii, M. Amemiya, K. Nakagawa, K. Ueda, and H. Katori: Opt. Lett. **34** (2009) 692.
61) H. Katori, T. Ido, and M. Kuwata-Gonokami: J. Phys. Soc. Jpn. **68** (1999) 2479.
62) T. Ido and H. Katori: Phys. Rev. Lett. **91** (2003) 053001.
63) A. V. Taichenachev, V. I. Yudin, C. W. Oates, C. W. Hoyt, Z. W. Barber, and L. Hollberg: Phys. Rev. Lett. **96** (2006) 083001.
64) A. Brusch, R. Le Targat, X. Baillard, M. Fouch, and P. Lemonde: Phys. Rev. Lett. **96** (2006) 103003.
65) Z. W. Barber, C. W. Hoyt, C. W. Oates, L. Hollberg, A. V. Taichenachev, and V. I. Yudin: Phys. Rev. Lett. **96** (2006) 083002.
66) X. Baillard, M. Fouche, R. Le Targat, P. G. Westergaard, A. Lecallier, Y. Le Coq, G. D. Rovera, S. Bize, and P. Lemonde: Opt. Lett. **32** (2007) 1812.
67) C. Lisdat, J. Winfred, T. Middelmann, F. Riehle, and U. Sterr: Phys. Rev. Lett. **103** (2009) 090801.
68) G. K. Campbell, M. M. Boyd, J. W. Thomsen, M. J. Martin, S. Blatt, M. D. Swallows, T. L. Nicholson, T. Fortier, C. W. Oates, S. A. Diddams, N. D. Lemke, P. Naidon, P. Julienne, J. Ye, and A. D. Ludlow: Science **324** (2009) 360.
69) K. Gibble: Phys. Rev. Lett. **103** (2009) 113202.
70) M. Takamoto and H. Katori: J. Phys. Soc. Jpn. **78** (2009) 013301.
71) A. Rauschenbeutel, H. Schadwinkel, V. Gomer, and D. Meschede: Opt. Commun. **148** (1998) 45.
72) T. Akatsuka, M. Takamoto, and H. Katori: Nat. Phys. **4** (2008) 954.
73) T. Akatsuka, M. Takamoto, and H. Katori: Phys. Rev. A **81** (2010) 023402.
74) M. Takamoto, H. Katori, S. I. Marmo, V. D. Ovsiannikov, and V. G. Pal'chikov: Phys. Rev. Lett. **102** (2009) 063002.
75) A. V. Taichenachev, V. I. Yudin, V. D. Ovsiannikov, V. G. Pal'chikov, and C. W. Oates: Phys. Rev. Lett. **101** (2008) 193601.
76) H. Katori, K. Hashiguchi, E. Yu. Il'inova, and V. D. Ovsiannikov: Phys. Rev. Lett. **103** (2009) 153004.
77) V. D. Ovsiannikov, V. G. Pal'chikov, H. Katori, and M. Takamoto: Quantum Electron. **36** (2006) 3.
78) C. Degenhardt, H. Stoehr, U. Sterr, F. Riehle, and C. Lisdat: Phys. Rev. A **70** (2004) 23414.
79) S. G. Porsev, A. Derevianko, and E. N. Fortson: Phys. Rev. A **69** (2004) 021403.
80) A. Ye and G. Wang: Phys. Rev. A **78** (2008) 014502.
81) R. Santra, E. Arimondo, T. Ido, C. H. Greene, and J. Ye: Phys. Rev. Lett. **94** (2005) 173002.
82) T. Hong, C. Cramer, W. Nagourney, and E. N. Fortson: Phys. Rev. Lett. **94** (2005) 50801.
83) V. D. Ovsiannikov, V. G. Pal'chikov, A. V. Taichenachev, V. I. Yudin, H. Katori, and M. Takamoto: Phys. Rev. A **75** (2007) 020501.
84) J.-P. Uzan: Rev. Mod. Phys. **75** (2003) 403.
85) E. J. Angstmann, V. A. Dzuba, and V. V. Flambaum: Phys. Rev. A **70** (2004) 014102.
86) I. Courtillot, A. Quessada, R. P. Kovacich, A. Brusch, D. Kolker, J. J. Zondy, G. D. Rovera, and P. Lemonde: Phys. Rev. A **68** (2003) 30501.
87) T. Mukaiyama, H. Katori, T. Ido, Y. Li, and M. Kuwata-Gonokami: Phys. Rev. Lett. **90** (2003) 113002.
88) M. M. Boyd, A. D. Ludlow, S. Blatt, S. M. Foreman, T. Ido, T. Zelevinsky, and J. Ye: Phys. Rev. Lett. **98** (2007) 083002.
89) X. Baillard, M. Fouche, R. Le Targat, P. G. Westergaard, A. Lecallier, F. Chapelet, M. Abgrall, G. D. Rovera, P. Laurent, P. Rosenbusch, S. Bize, G. Santarelli, A. Clairon, P. Lemonde, G. Grosche, B. Lipphardt, and H. Schnatz: Eur. Phys. J. D **48** (2008) 11.
90) Bureau International des Poids et Mesures (BIPM), Circular T [http://www1.bipm.org/en/scientific/tai/time_ftp.html].
91) C. W. Hoyt, Z. W. Barber, C. W. Oates, T. M. Fortier, S. A. Diddams, and L. Hollberg: Phys. Rev. Lett. **95** (2005) 083003.
92) N. Poli, Z. W. Barber, N. D. Lemke, C. W. Oates, L. S. Ma, J. E. Stalnaker, T. M. Fortier, S. A. Diddams, L. Hollberg, J. C. Bergquist, A. Brusch, S. Jefferts, T. Heavner, and T. Parker: Phys. Rev. A **77** (2008) 050501(R).
93) Z. W. Barber, J. E. Stalnaker, N. D. Lemke, N. Poli, C. W. Oates, T. M. Fortier, S. A. Diddams, L. Hollberg, C. W. Hoyt, A. V. Taichenachev, and V. I. Yudin: Phys. Rev. Lett. **100** (2008) 103002.
94) F.-L. Hong, H. Inaba, K. Hosaka, M. Yasuda, and A. Onae: Opt. Express **17** (2009) 1652.
95) P. Gill and F. Riehle: Proc. EFTF, 2006, p. 282.
96) J. Millo, D. V. Magalhaes, C. Mandache, Y. Le Coq, E. M. L. English, P. G. Westergaard, J. Lodewyck, S. Bize, P. Lemonde, and G. Santarelli: Phys. Rev. A **79** (2009) 053829.
97) H. J. Kimble, B. L. Levz, and J. Ye: Phys. Rev. Lett. **101** (2008) 260602.
98) H. Schnatz, O. Terra, K. Predehl, T. Feldmann, T. Legero, B. Lipphardt, U. Sterr, G. Grosche, K. Predehl, T. W. Hänsch, R. Holzwarth, Th. Udem, Z. Lu, L. Wang, W. Ertmer, J. Friebe, A. Pape, E.-M. Rasel, M. Riedmann, and T. Wübbena: Proc. EFTF, 2009, ID7120.

Feng-Lei Hong received the B.S., M.S., and Ph. D. degrees in physics from the University of Tokyo, Tokyo, Japan in 1987, 1989, and 1992, respectively. After a two-year postdoctoral appointment working on laser and microwave double-resonance spectroscopy of Rydberg atoms at RIKEN, Japan, in 1994, he joined the National Research Laboratory of Metrology (NRLM), now named as the National Metrology Institute of Japan (NMIJ), the National Institute of Advanced Industrial Science and Technology (AIST), Tsukuba, Japan, where he is a Group Leader. His current research interests include high-resolution laser spectroscopy, laser frequency stabilization, optical frequency standards, optical frequency measurement, and ultrafast optics. As a Visiting Member, he was with JILA, Boulder, CO of the National Institute of Standards and Technology (NIST), Boulder, CO, and the University of Colorado, Boulder, CO from 1997 to 1999. Dr. Hong received the JSPE Paper Award in 2003 and the Prize for Science and Technology by the Minister of Education, Culture, Sports, Science and Technology in 2008. He is a member of the Japan Society of Applied Physics, the Physical Society of Japan, and the Optical Society of America.

Hidetoshi Katori was born in Tokyo, Japan, in 1964. He received the B. Eng. in Applied Physics from The University of Tokyo in 1988, and M. Eng. and D. Eng. in Applied Physics from the Graduate School of Engineering, The University of Tokyo in 1990 and 1994. From 1994 to 1997, he worked at Max Planck Institute for Quantum Optics in Garching, Germany, as a visiting scientist. He joined Engineering Research Institute, The University of Tokyo in 1999. Since then he has been engaged in the precision measurements with ultracold atoms. He is a professor in the department of applied physics, graduate school of engineering, The University of Tokyo, and currently serves as a research director of CREST (2005–2010), Japan Science and Technology Agency (JST). He was awarded the first JSPS Prize, European Time and Frequency Award, and The Julius Springer Prize for Applied Physics in 2005, Marubun special science award and IBM Japan Science Prize in 2006, Rabi Award in 2008, and Ichimura Academic Award, Special Prize in 2010.

